An efficient kinetic modeling in plasmas by using the AWBS transport equation

Authors[a,1]

[a] *Centre Lasers Intenses et Applications, Universite de Bordeaux-CNRS-CEA, UMR 5107, F-33405 Talence, France*

Abstract

Keywords: kinetics; hydrodynamics; nonlocal electron transport; laser-heated plasmas.

*Corresponding author.
E-mail address: milan.holec@u-bordeaux.fr

1. Introduction

2. The AWBS nonlocal transport model

$$\frac{\partial f}{\partial t} + \boldsymbol{v} \cdot \nabla_{\boldsymbol{x}} f + \tilde{\boldsymbol{E}} \cdot \nabla_{\boldsymbol{v}} f = v \frac{\nu_e}{2} \frac{\partial}{\partial v} \left(f - f_M \right) + \frac{\nu_{ei} + \frac{\nu_e}{2}}{2} \frac{\partial^2 f}{\partial \boldsymbol{n}^2}, \tag{1}$$

[1]

3. BGK, AWBS, and Fokker-Planck models in local diffusive regime

We can try to find an approximate solution while using the first term of expansion in λ_{ei} and μ as

$$\tilde{f}(z, v, \mu) = f^0(z, v) + f^1(z, v) \lambda_{ei} \mu, \tag{2}$$

where $\lambda_{ei} = \frac{v^4}{\bar{Z} n_e \Gamma^{ee}}$.

3.1. The BGK local diffusive electron transport

$$\mu \left(\frac{\partial f}{\partial z} + \frac{\tilde{E}_z}{v} \frac{\partial f}{\partial v} \right) + \frac{\tilde{E}_z (1 - \mu^2)}{v^2} \frac{\partial f}{\partial \mu} = \frac{f - f_M}{\lambda_e} + \frac{1}{2 \lambda_{ei}} \frac{\partial}{\partial \mu} (1 - \mu^2) \frac{\partial f}{\partial \mu}, \tag{3}$$

$$f^0 = f_M + \frac{1}{v} f^1 \bar{Z} \lambda_{ei}^2, \tag{4}$$

$$f^1 = - \frac{\bar{Z}}{\bar{Z} + 1} \left[\frac{\partial f^0}{\partial z} + \frac{\tilde{E}_z}{v} \frac{\partial f^0}{\partial v} \right], \tag{5}$$

$$f = f_M - \frac{\bar{Z}}{\bar{Z} + 1} \left[\frac{1}{\rho} \frac{\partial \rho}{\partial z} + \left(\frac{v^2}{2 v_{th}^2} - \frac{3}{2} \right) \frac{1}{T} \frac{\partial T}{\partial z} - \frac{\tilde{E}_z}{v_{th}^2} \right] f_M \lambda_{ei} \mu,$$

and when holds $\boldsymbol{j} \equiv q_e \int \boldsymbol{v} f \, \mathrm{d}\boldsymbol{v} = \boldsymbol{0} \rightarrow \tilde{\boldsymbol{E}} = v_{th}^2 \left(\frac{\nabla \rho}{\rho} + \frac{5}{2} \frac{\nabla T}{T} \right)$, i.e. the electric field $\tilde{E}_z$ obeying the zero current condition leads to

$$f = f_M - \frac{\bar{Z}}{\bar{Z} + 1} \left(\frac{v^2}{2 v_{th}^2} - 4 \right) \frac{1}{T} \frac{\partial T}{\partial z} f_M \lambda_{ei} \mu,$$

3.2. The AWBS diffusive electron transport

$$\mu\left(\frac{\partial f}{\partial z}+\frac{\tilde{E}_z}{v}\frac{\partial f}{\partial v}\right)+\frac{\tilde{E}_z(1-\mu^2)}{v^2}\frac{\partial f}{\partial \mu}=$$
$$\frac{v}{2\lambda_e}\frac{\partial}{\partial v}\left(f-f_M\right)+\frac{1}{2}\left(\frac{1}{\lambda_{ei}}+\frac{1}{2\lambda_e}\right)\frac{\partial}{\partial \mu}(1-\mu^2)\frac{\partial f}{\partial \mu}, \quad (6)$$

$$\begin{aligned}\frac{\partial}{\partial v}\left(f^0-f_M\right) &= \frac{1}{v^2}f^1\bar{Z}\lambda_{ei}^2, \qquad (7)\\ \frac{v}{\bar{Z}\lambda_{ei}}\frac{\partial(f^1\lambda_{ei})}{\partial v}-\frac{\bar{Z}+1}{\bar{Z}}f^1 &= \frac{\partial f^0}{\partial z}+\frac{\tilde{E}_z}{v}\frac{\partial f^0}{\partial v}\end{aligned}$$

$$\frac{\partial f^1}{\partial v}+\frac{1}{v}(3-\bar{Z})f^1=\frac{\bar{Z}}{v}\left(\frac{1}{\rho}\frac{\partial \rho}{\partial z}+\left(\frac{v^2}{2v_{th}^2}-\frac{3}{2}\right)\frac{1}{T}\frac{\partial T}{\partial z}-\frac{\tilde{E}_z}{v_{th}^2}\right)f_M. \quad (8)$$

3.3. The Fokker-Planck diffusive electron transport

$$\mu\left(\frac{\partial f}{\partial z}+\frac{\tilde{E}_z}{v}\frac{\partial f}{\partial v}\right)+\frac{\tilde{E}_z(1-\mu^2)}{v^2}\frac{\partial f}{\partial \mu}=$$
$$\frac{\Gamma^{ee}}{v}\left(4\pi f^2+\frac{\nabla_{\boldsymbol{v}}\nabla_{\boldsymbol{v}}f:\nabla_{\boldsymbol{v}}\nabla_{\boldsymbol{v}}g}{2}\right)+\frac{1}{\lambda_{ei}}\frac{\partial}{\partial \mu}(1-\mu^2)\frac{\partial f}{\partial \mu},$$

where $g(\boldsymbol{v})=\int|\boldsymbol{v}-\boldsymbol{v}^*|f(\boldsymbol{v}^*)\,\mathrm{d}\boldsymbol{v}^*$ is the Rosenbluth potential [2]. Since we are interested in the approximate solution in the diffusive regime, it is convenient to use a low anisotropy approximation $\tilde{g}=g^0(f^0)+g^1(f^1)\lambda_{ei}(v)\mu$, which arises from Eq. 45 in [2].

$$\Gamma^{ee}\left(4\pi\tilde{f}^2+\frac{\nabla_{\boldsymbol{v}}\nabla_{\boldsymbol{v}}\tilde{f}:\nabla_{\boldsymbol{v}}\nabla_{\boldsymbol{v}}\tilde{g}}{2}\right)=\Gamma^{ee}\left(4\pi {f^0}^2+\frac{1}{2}\frac{\partial^2 f^0}{\partial v^2}\frac{\partial^2 g^0}{\partial v^2}+\frac{1}{v^2}\frac{\partial f^0}{\partial v}\frac{\partial g^0}{\partial v}\right)$$
$$+\frac{\mu}{n_e}\left[8\pi f^0 f^1 v^4-v\left(\frac{\partial f^0}{\partial v}g^1+\frac{\partial g^0}{\partial v}f^1\right)+\frac{1}{v^2}\left(\frac{\partial f^0}{\partial v}\frac{\partial(g^1v^4)}{\partial v}+\frac{\partial g^0}{\partial v}\frac{\partial(f^1v^4)}{\partial v}\right)\right.$$
$$\left.+\frac{1}{2}\left(\frac{\partial^2 f^0}{\partial v^2}\frac{\partial^2(g^1v^4)}{\partial v^2}+\frac{\partial^2 g^0}{\partial v^2}\frac{\partial^2(f^1v^4)}{\partial v^2}\right)\right]+O(\lambda_{ei}^2,\mu^2)$$

	$\bar{Z}=1$	$\bar{Z}=2$	$\bar{Z}=4$	$\bar{Z}=16$	$\bar{Z}=116$
$\bar{\Delta}\boldsymbol{q}_{AWBS}$	0.057	0.004	0.038	0.049	0.004

Table 1: Relative error $\bar{\Delta}\boldsymbol{q}_{AWBS} = |\boldsymbol{q}_{AWBS} - \boldsymbol{q}_{SH}|/\boldsymbol{q}_{SH}$ of the AWBS kinetic model equation (1) showing the discrepancy (maximum around 5%) with respect to the original solution of the heat flux given by Spitzer and Harm [5].

$$\Gamma^{ee}\left(4\pi f^{0^2} + \frac{1}{2}\frac{\partial^2 f^0}{\partial v^2}\frac{\partial^2 g^0}{\partial v^2} + \frac{1}{v^2}\frac{\partial f^0}{\partial v}\frac{\partial g^0}{\partial v}\right) = \frac{1}{v^2} f^1 \bar{Z}\lambda_{ei}^2, \tag{9}$$

$$\begin{aligned}\frac{1}{2}\left(\frac{\partial^2 f_M}{\partial v^2}\frac{\partial^2(g^1v^4)}{\partial v^2} + \frac{\partial^2 g_M}{\partial v^2}\frac{\partial^2(f^1v^4)}{\partial v^2}\right) + \frac{1}{v^2}\left(\frac{\partial f_M}{\partial v}\frac{\partial(g^1v^4)}{\partial v} + \frac{\partial g_M}{\partial v}\frac{\partial(f^1v^4)}{\partial v}\right)\\ - v\left(\frac{\partial f_M}{\partial v}g^1 + \frac{\partial g_M}{\partial v}f^1\right) + 8\pi f_M f^1 v^4 - n_e v f^1 = n_e v\frac{\partial f_M}{\partial z} + n_e\tilde{E}_z\frac{\partial f_M}{\partial v},\end{aligned} \tag{10}$$

$$f_1(v,\mu) = \mu\frac{m_e^2}{4\pi e^4 \ln\Lambda}\frac{v_{2th}^4}{\bar{Z}}\left(2d_T(v/v_{2th}) + \frac{3}{2}\frac{\gamma_T}{\gamma_E}d_E(v/v_{2th})\right)\frac{f_M(v)}{n_e}\frac{\nabla T}{T}, \tag{11}$$

where $d_T(x) = \bar{Z}D_T(x)/B$ and $d_E(x) = \bar{Z}D_E(x)/A$ are represented by numerical values in TABLE I and TABLE II in [5], respectively.

[2], [3], [4]

3.4. Summary of BGK, AWBS, and Fokker-Planck diffusion

4. Benchmarking the AWBS nonlocal transport model

4.1. C7

In order to eliminate the dimensions of the above transport problem the first-two-moment model based on approximation

$$f = \frac{f_0}{4\pi} + \frac{3}{4\pi}\boldsymbol{n}\cdot\boldsymbol{f_1},$$

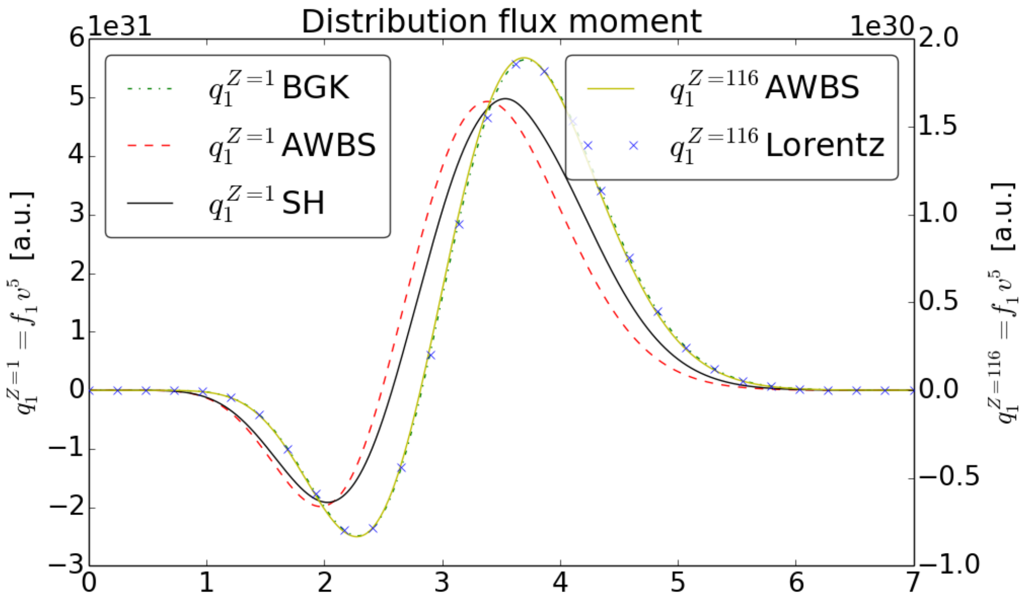

Figure 1: The flux velocity moment of the anisotropic part of the electron distribution function in low $Z = 1$ and high $Z = 116$ plasmas in diffusive regime.

can be adopted and reads

$$\begin{aligned} v\frac{\nu_e}{2}\frac{\partial}{\partial v}\left(f_0 - 4\pi f_M\right) &= v\nabla\cdot\boldsymbol{f_1} + \tilde{\boldsymbol{E}}\cdot\frac{\partial \boldsymbol{f_1}}{\partial v} + \frac{2}{v}\tilde{\boldsymbol{E}}\cdot\boldsymbol{f_1}, \\ v\frac{\nu_e}{2}\frac{\partial \boldsymbol{f_1}}{\partial v} - \left(\nu_{ei} + \frac{\nu_e}{2}\right)\boldsymbol{f_1} &= \frac{v}{3}\nabla f_0 + \frac{\tilde{\boldsymbol{E}}}{3}\frac{\partial f_0}{\partial v}, \end{aligned}$$

$$\boldsymbol{q}_c \equiv q_e \int_v \left(\frac{\nu_e v^2}{\nu_{ei} + \frac{\nu_e}{2}}\frac{\partial \boldsymbol{f_1}}{\partial v} - \frac{v^2}{3\left(\nu_{ei} + \frac{\nu_e}{2}\right)}\nabla f_0 - \frac{v}{3\left(\nu_{ei} + \frac{\nu_e}{2}\right)}\frac{\partial f_0}{\partial v}\tilde{\boldsymbol{E}}\right) v^2\, \mathrm{d}v = 0,$$

4.1.1. Nonlocal electric field treatment

$$\left(v\frac{\nu_e}{2} - \frac{2\tilde{E}_z^2}{3v\nu_e}\right)\frac{\partial f_{1_z}}{\partial v} = \\ \frac{2\tilde{E}_z}{3\nu_e}\frac{\partial f_{1_z}}{\partial z} + \frac{4\pi\tilde{E}_z}{3}\frac{\partial f_M}{\partial v} + \frac{v}{3}\frac{\partial f_0}{\partial z} + \left(\frac{4\tilde{E}_z^2}{3v^2\nu_e} + \left(\nu_{ei} + \frac{\nu_e}{2}\right)\right) f_{1_z},$$

Kn	10^{-3}	5×10^{-3}	10^{-2}	5×10^{-2}	10^{-1}
$v_{lim}^{Z=1}/v_{th}$	21.6	9.8	7.0	3.8	3.1
$v_{lim}^{Z=10}/v_{th}$	6.7	3.4	2.6	1.6	1.3

Table 2: $\sqrt{3}v\frac{\nu_e}{2} > |\tilde{\boldsymbol{E}}|$.

$$
\begin{aligned}
|\tilde{\boldsymbol{E}}_{red}| &= v\frac{\nu_e}{2}, \\
\nu_{ei}^{E} &= \frac{|\tilde{\boldsymbol{E}}| - |\tilde{\boldsymbol{E}}_{red}|}{v},
\end{aligned}
$$

where $\omega_{red} = |\tilde{\boldsymbol{E}}_{red}|/|\tilde{\boldsymbol{E}}|$.

P1 approximation equivalent

$$
f = \frac{4\pi f_M + \delta f_0}{4\pi} + \frac{3}{4\pi}\boldsymbol{n}\cdot\boldsymbol{f_1}. \tag{12}
$$

where the moment model reads

$$
\begin{aligned}
v\frac{\nu_e}{2}\frac{\partial \delta f_0}{\partial v} &= v\nabla\cdot\boldsymbol{f_1} + \tilde{\boldsymbol{E}}\cdot\left(\omega_{red}\frac{\partial \boldsymbol{f_1}}{\partial v} + \frac{2}{v}\boldsymbol{f_1}\right), \\
v\frac{\nu_e}{2}\frac{\partial \boldsymbol{f_1}}{\partial v} &= \left(\nu_{ei} + \nu_{ei}^{E} + \frac{\nu_e}{2}\right)\boldsymbol{f_1} + \frac{v}{3}\nabla\left(4\pi f_M + \delta f_0\right) \\
&\quad + \frac{\tilde{\boldsymbol{E}}}{3}\left(4\pi\frac{\partial f_M}{\partial v} + \omega_{red}\frac{\partial \delta f_0}{\partial v}\right),
\end{aligned}
$$

$$
\tilde{\boldsymbol{E}} = \frac{\int_v \left(\frac{\frac{\nu_e}{2}v^2}{\nu_{ei}+\nu_{ei}^{E}+\frac{\nu_e}{2}}\frac{\partial \boldsymbol{f_1}}{\partial v} - \frac{v^2}{3\left(\nu_{ei}+\nu_{ei}^{E}+\frac{\nu_e}{2}\right)}\nabla\left(4\pi f_M + \delta f_0\right)\right) v^2\,\mathrm{d}v}{\int_v \frac{v}{3\left(\nu_{ei}+\nu_{ei}^{E}+\frac{\nu_e}{2}\right)}\left(4\pi\frac{\partial f_M}{\partial v} + \omega_{red}\frac{\partial \delta f_0}{\partial v}\right) v^2\,\mathrm{d}v},
$$

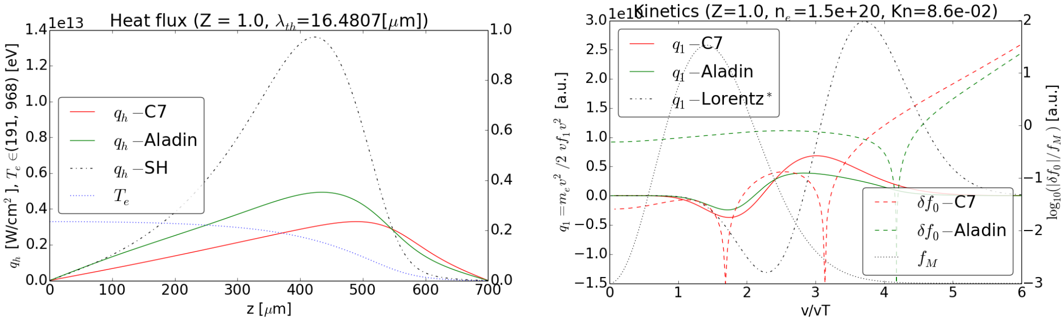

Figure 2: Snapshot 20 ps. Left: correct steady solution of heat flux. Right: Aladins results are need to added.

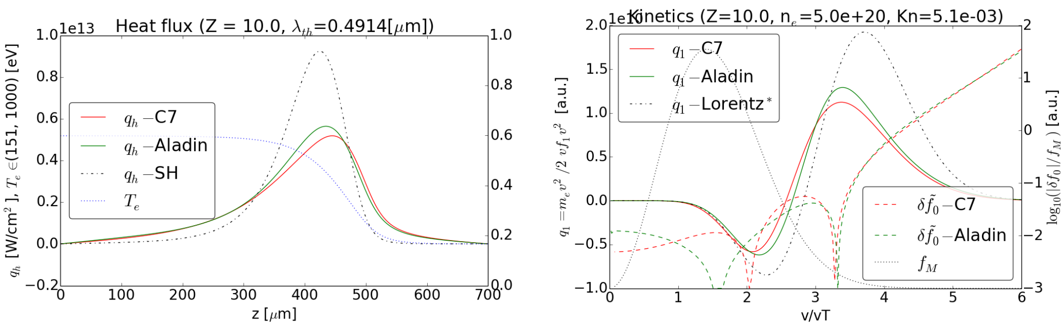

Figure 3: Snapshot 12 ps. Left: correct steady solution of heat flux. Right: correct comparison to kinetic profiles at point 442 μm by Aladin.

4.2. Aladin

4.3. Impact

4.4. Calder

4.5. Simulation results

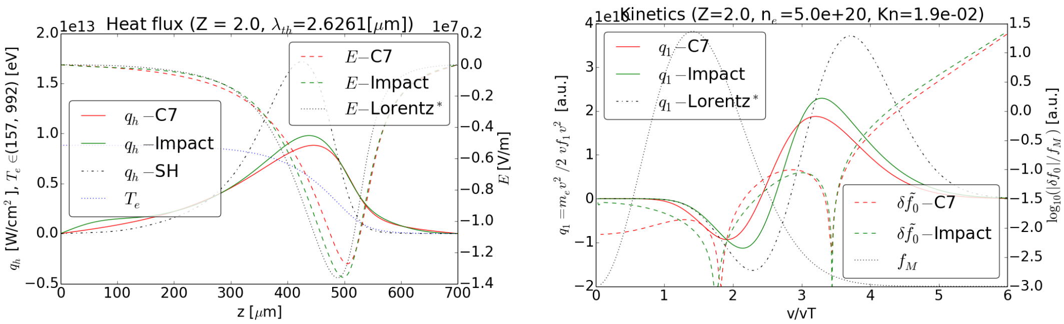

Figure 4: Snapshot 12 ps. Left: correct steady solution of heat flux. Right: correct comparison to kinetic profiles at point 437 μm by Impact.

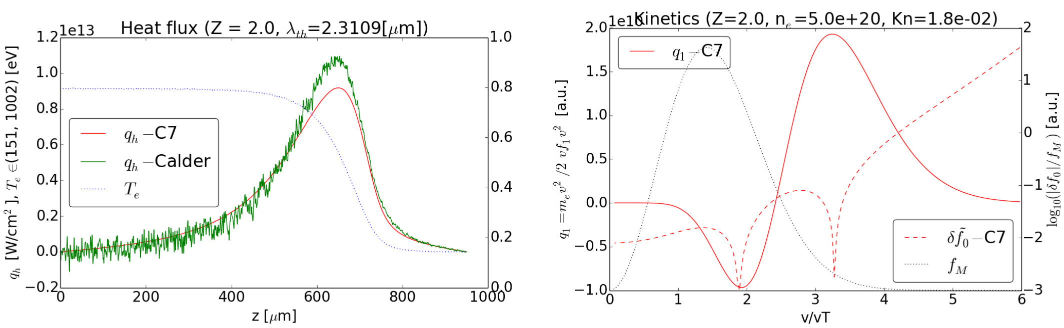

Figure 5: Snapshot 11 ps. Left: correct steady solution of heat flux. Right: Kinetic profiles at point of maximum flux by C7. Kinetics profiles by CALDER should be added.

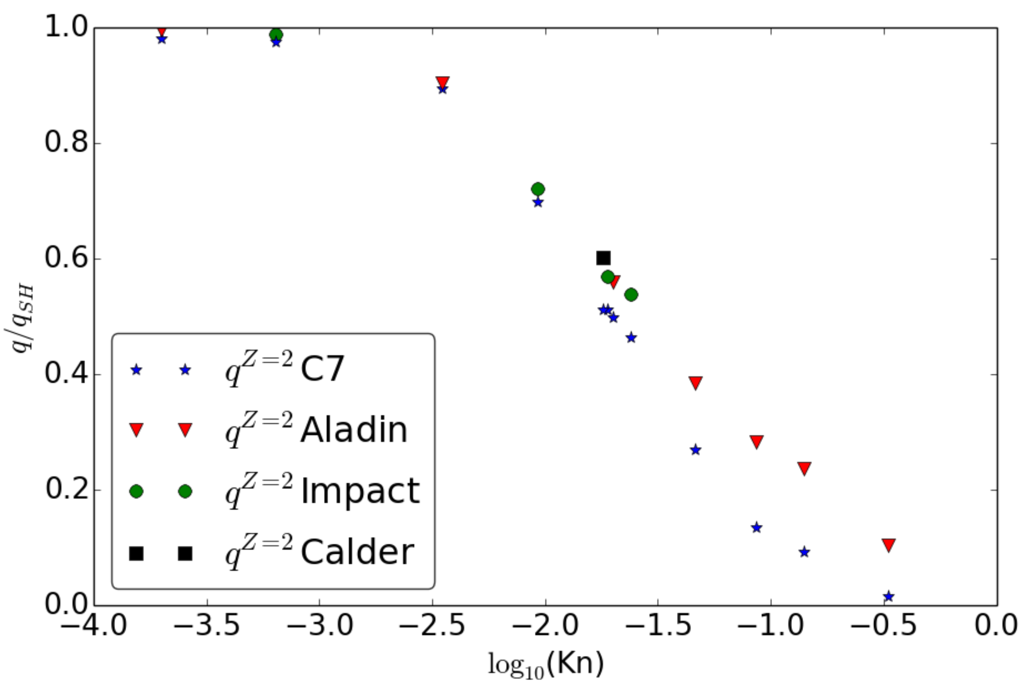

Figure 6: Simulation results for the case $Z = 2$ computed by C7/Aladin/Impact/Calder. Every point corresponds to the maximum heat flux in a "tanh" temperature simulation, which can be characterized by Kn. The range of $\log_{10}(\mathrm{Kn}) \in (-0.5, -3.5)$ can be expressed as equivalent to the electron density approximate range $\mathrm{n}_e \in (5e19, 3.5e22)$ of the 50 μm slope tanh case.

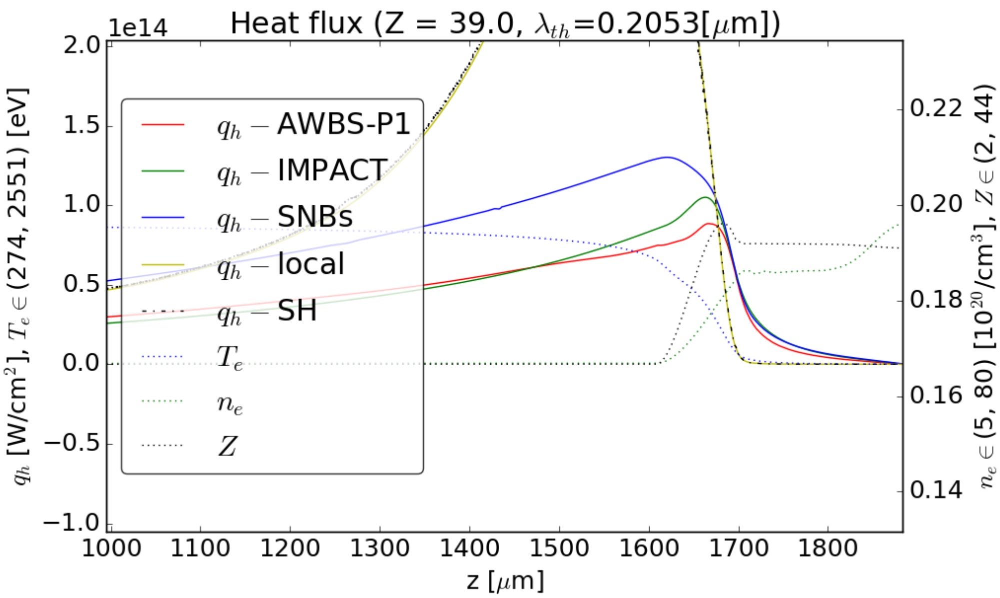

Heat flux (Z = 39.0, λ_{th}=0.2053[μm])
1e14
q_h [W/cm^2], $T_e \in$ (274, 2551) [eV]
$n_e \in$ (5, 80) [10^{20}/cm^3], $Z \in$ (2, 44)
z [μm]
$q_h -$ AWBS-P1
$q_h -$ IMPACT
$q_h -$ SNBs
$q_h -$ local
$q_h -$ SH
T_e
n_e
Z

Figure 7:

5. Conclusions

[1] Nathaniel J. Fisch. Theory of current drive in plasmas. Rev. Mod. Phys., 59(1):175234, Jan 1987.

[2] Marshall N. Rosenbluth, William M. MacDonald, and David L. Judd. Fokker-planck equation for an inverse-square force. Phys. Rev., 107(1):16, Jul 1957.

[3] Longmire, Conrad L. : Elementary Plasma Physics. Intersci. Pub., 1963.

[4] I.P. Shkarofsky, T.W. Johnston, T.W. Bachynski, The Particle Kinetics of Plasmas, Addison-Wesley, Reading, MA, 1966.

[5] SH 1953.